THE JOURNAL OF BIOLOGICAL CHEMISTRY VOL. 286, NO. 12, pp. 10341–10355, March 25, 2011
Printed in the U.S.A.

Gcn1 and Actin Binding to Yih1

*IMPLICATIONS FOR ACTIVATION OF THE eIF2 KINASE GCN2**

Received for publication, August 4, 2010, and in revised form, January 12, 2011 Published, JBC Papers in Press, January 14, 2011, DOI 10.1074/jbc.M110.171587

Evelyn Sattlegger[‡§1], João A. R. G. Barbosa[¶2], Maria Carolina S. Moraes[‖3,4], Rafael M. Martins[‖3], Alan G. Hinnebusch[§], and Beatriz A. Castilho[‖]

From the [‡]Institute of Natural Sciences, Massey University, Auckland 0745, New Zealand, the [‖]Departamento de Microbiologia, Imunologia, e Parasitologia, Universidade Federal de São Paulo, São Paulo, SP 04023-062, Brazil, the [§]Laboratory of Gene Regulation and Development, NICHD, National Institutes of Health, Bethesda, Maryland 20892, and the [¶]Center for Structural Molecular Biology, Brazilian Synchrotron Light Laboratory, C.P. 6192, 13083-970 Campinas, Brazil

Yeast Yih1 protein and its mammalian ortholog IMPACT, abundant in neurons, are inhibitors of Gcn2, a kinase involved in amino acid homeostasis, stress response, and memory formation. Like Gcn2, Yih1/IMPACT harbors an N-terminal RWD domain that mediates binding to the Gcn2 activator Gcn1. Yih1 competes with Gcn2 for Gcn1 binding, thus inhibiting Gcn2. Yih1 also binds G-actin. Here, we show that Yih1-actin interaction is independent of Gcn1 and that Yih1-Gcn1 binding does not require actin. The Yih1 RWD (residues 1–132) was sufficient for Gcn2 inhibition and Gcn1 binding, but not for actin binding, showing that actin binding is dispensable for inhibiting Gcn2. Actin binding required Yih1 residues 68–258, encompassing part of the RWD and the C-terminal "ancient domain"; however, residues Asp-102 and Glu-106 in helix3 of the RWD were essential for Gcn1 binding and Gcn2 inhibition but dispensable for actin binding. Thus, the Gcn1- and actin-binding sites overlap in the RWD but have distinct binding determinants. Unexpectedly, Yih1 segment 68–258 was defective for inhibiting Gcn2 even though it binds Gcn1 at higher levels than does full-length Yih1. This and other results suggest that Yih1 binds with different requirements to distinct populations of Gcn1 molecules, and its ability to disrupt Gcn1-Gcn2 complexes is dependent on a complete RWD and hindered by actin binding. Modeling of the ancient domain on the bacterial protein YigZ showed peculiarities to the eukaryotic and prokaryotic lineages, suggesting binding sites for conserved cellular components. Our results support a role for Yih1 in a cross-talk between the cytoskeleton and translation.

In all eukaryotes, phosphorylation of the α-subunit of translation initiation factor 2 (eIF2α)[5] is a major mechanism for the regulation of protein synthesis in response to a variety of environmental or intracellular stresses. This event leads to general translation inhibition at the same time that it allows for increased translation of specific messages, such as *GCN4* in yeast and *ATF4* in mammals. These code for transcription factors that activate a network of genes aimed at cell recovery from the initial stress (1).

Gcn2, the sole eIF2α kinase in the yeast *Saccharomyces cerevisiae*, is activated by amino acid starvation and imbalance and other stresses (2). Gcn2 is a highly conserved protein found in all eukaryotic organisms, and in mammals it has been implicated in additional functions such as modulating the immune system, feeding behavior, and memory formation (3–6). Gcn2 is composed of five distinct functional domains. At its N terminus, a region called the RWD domain (from its presence in RING finger proteins, WD-repeat-containing proteins, and yeast DEAD-like helicases) (7) binds directly to the activator protein Gcn1 (8, 9). Its kinase catalytic domain is found in the center of the protein. Between the RWD domain and the kinase domain resides a pseudo-kinase domain, identifiable by characteristic but incomplete protein kinase sequences, with no well defined function. A domain C-terminal to the kinase region has similarity to histidyl-tRNA synthetases (HisRS) and binds uncharged tRNAs that accumulate under amino acid starvation conditions, signaling for the activation of the catalytic domain (2). At the C terminus, Gcn2 contains a region required for its association with ribosomes and for dimerization (2).

Gcn1 is necessary for the activation of Gcn2, and it binds the ribosome and Gcn2 through distinct regions (8, 10–12). We have proposed that Gcn1 is directly involved in facilitating the transfer of uncharged tRNAs from the decoding site A of the ribosome to the HisRS-like domain of Gcn2 when both Gcn1 and Gcn2 are associated with translating ribosomes (8, 13). The C-terminal region of Gcn1 binds directly to the RWD domain of Gcn2, and this interaction is dependent on residue Arg-2259 in Gcn1 (8). Mutation of this amino acid in Gcn1 disables Gcn2 activation *in vivo*, and this is overcome by Gcn2 overexpression, supporting the idea that direct Gcn1-Gcn2 interaction is essential for Gcn2 activation (8).

* This work was supported, in whole or in part, by National Institutes of Health Intramural Research Program. This work was also supported in part by the Health Research Council of New Zealand Emerging Researcher First Grant, Auckland Medical Research Foundation, Massey University Research and Technician's Fund, Maurice and Phyllis Paykel Trust (to E. S.), and a grant from Fundação de Amparo a Pesquisa do Estado de São Paulo (to B. A. C.).

[1] To whom correspondence should be addressed: Institute of Natural Sciences, Massey University, Private Bag 102 904, North Shore Mail Centre, Albany, Auckland 0745, New Zealand. Tel.: 64-9-414-0800 (Ext. 9665 or 41126); Fax: 64-9-441-8142; E-mail: e.sattlegger@massey.ac.nz.

[2] Present address: Pós-Graduação em Ciências Genômicas e Biotecnologia, Universidade Católica de Brasília, 70790-160, Brasília, DF, Brazil.

[3] Supported by a doctoral fellowship from Fundação de Amparo a Pesquisa do Estado de São Paulo.

[4] Present address: Dept. de Microbiologia, Instituto de Ciências Biomédicas, Universidade de São Paulo, São Paulo, SP 05508-902, Brazil.

[5] The abbreviations used are: eIF2, translation initiation factor 2; 3AT, 3-amino-2,4-triazole.

The three-dimensional structure of the RWD domain of mammalian Gcn2 has been solved by NMR (14). It represents a unique fold, albeit with some similarity with the mammalian E2 ubiquitin-conjugating enzyme UBC9 and with a yeast E2 variant protein (UEV), Mms2. Residues that may contact Gcn1 have been proposed based on their localization on the surface of the structure and on their conservation unique to Gcn2 but not to E2 or UEV (14).

The yeast Yih1 protein was identified as an ortholog of the mouse IMPACT (imprinted and ancient) protein that is expressed preferentially in neurons (15, 16, 17). For both proteins, the C-terminal region has similarity to the N-terminal half of the YigZ family of prokaryotic proteins of unknown function. Because orthologous domains are found throughout the bacterial, archaeal, and eukaryotic kingdoms, this region of Yih1/IMPACT has been termed the "ancient domain" (17).

Yih1 contains an RWD domain, also known as the GI domain, localized in its N-terminal half (9). Given its similarity to the N-terminal Gcn2 RWD domain known to be required for Gcn1 interaction, Kubota *et al.* (9) proposed that Yih1 interacts with Gcn1. The segment of yeast Gcn2 comprising the RWD domain (residues 1–125) was shown to bind to Gcn1, and a two-hybrid interaction of Yih1 and Gcn1 was reported as unpublished observations. We have provided several lines of evidence for Yih1-Gcn1 interaction *in vivo* and *in vitro* (18), and we have shown that Yih1 binds directly to the C-terminal region of Gcn1 encompassing amino acids 2052–2428 (18). Kubota *et al.* (9) showed that overexpression of Yih1 results in a growth defect under amino acid starvation conditions, from which it was proposed that Yih1 inhibits Gcn2 activation by competing with Gcn2 for Gcn1 binding (9). We provided several lines of genetic and physical evidence unambiguously demonstrating that overexpressed Yih1 in fact does reduce Gcn1-Gcn2 complex formation through a competition mechanism, thereby inhibiting Gcn2 activation. We have also shown that Yih1 overexpression leads to reduced eIF2α phosphorylation, that Arg-2259 in Gcn1 is required for Yih1-Gcn1 interaction as found for Gcn2, and that co-overexpression of Gcn2 reverted the phenotype associated with Yih1 overexpression (18). In addition, we have shown that IMPACT substitutes for Yih1 function in yeast and that IMPACT also binds to yeast Gcn1, dependent on residue Arg-2259, and binds to Gcn1 in mammalian cells. Furthermore, IMPACT overexpression in mammalian cells inhibits Gcn2 activation, suggesting that Yih1 and IMPACT proteins are functional homologs (15). In mammals, IMPACT is expressed preferentially in neurons (15, 16). Interestingly, Gcn2 has been implicated in long term potentiation and memory in mice (3), leading us to propose that IMPACT may be involved in brain-related functions as well.

We have uncovered that endogenous Yih1 associates with monomeric actin (G-actin) (18). Reduced actin levels lead to the inability of cells to respond to amino acid starvation, and this was partially reverted by deleting *YIH1*, suggesting that actin modulates Gcn2 down-regulation via Yih1, and thus implicating Yih1 in cross-talk between translation and the cytoskeleton (18). Curiously, deletion of *YIH1* does not lead to increased Gcn2 activity, suggesting that Yih1 inhibits Gcn2 in a temporally or spatially restricted manner when/where Gcn2 activation is deleterious to the cell (18). We proposed a model for Yih1 function in which Yih1 resides in the cell in an inactive Yih1-G-actin complex, and when released from actin Yih1 then competes with Gcn2 for Gcn1 binding. One possibility is that free Yih1 accumulates near the bud tip, where actin is mainly polymerized in its filamentous form (F-actin) or assembled in actin patches, leading to locally reduced Gcn2 activation. As a result, robust translation is ensured at a site where high levels of protein synthesis are needed for the growing bud (18).

Given the relevance of Yih1/IMPACT in controlling a crucial and multifunctional signal-transducing mechanism that is conserved from yeast to mammals, a detailed understanding of the interaction between Yih1 and Gcn1 and actin is essential. In this study, we show that Yih1 binds directly to Gcn1 *in vitro* and that Yih1 can bind independently to actin and Gcn1 *in vivo*. We demonstrate that the RWD domain is sufficient to bind Gcn1 and inhibit Gcn2 but fails to bind actin, showing that actin binding is dispensable for inhibiting Gcn2. Rather, we obtained evidence that actin binding hinders this regulatory function of Yih1. Actin binding requires the C-terminal portion of the RWD in addition to the ancient domain, but we found that Gcn1 and actin have distinct binding determinants in the RWD. Surprisingly, the C-terminal segment of the RWD can bind Gcn1 but does not inhibit Gcn2, and possible mechanisms are discussed to explain the requirement for an intact RWD in displacing Gcn1 from Gcn1-Gcn2 complexes. Finally, we highlight a conserved putative interaction surface characteristic of ancient domains that harbors determinants characteristic to either eukaryotes or prokaryotes.

EXPERIMENTAL PROCEDURES

Strains and Plasmids—The *Escherichia coli* strain used in this study was BL21(DE3) (Novagen). Yeast strains used were wild-type H1511 (MATα, *ura3-52*, *trp1-63*, *leu2-3*, *leu2-112*, *GAL2*$^+$) (19) and its isogenic derivative deleted for *GCN1* (H2556).[6] *YIH1* was deleted in the H1511 strain using PCR-based published procedures (20), resulting into the *yih1*Δ strain ESY11001b.

Plasmids used and constructed in this study are listed in Table 1. Vectors used were pES128-9 (8), the pGEX-6p series (GE Healthcare), and pET-28a (Stratagene). The Yih1 fragments fused to GST were constructed as reported for pES187-B1 (10), except that the PCR primers used only amplified the regions encoding for the desired fraction of Yih1. Point mutations and thus amino acid substitutions were introduced into Yih1 via standard PCR methods as done previously (10). The base substitutions were as follows: E87A, GAA to GCC substitution; D90A, GAC to GCC; D102A, GAC to GCC; E106A, GAA to GCC. Outside primers for amplifying the entire *YIH1* allele and for cloning the PCR product into pES128-9 were the same as the ones used for the construction of pES187-B1 (18).

In Vitro Yih1-Gcn1 Binding Studies—GST fusion proteins were expressed, immobilized, and washed on glutathione-based affinity resin as published previously (8). Purified His_6-tagged Yih1, in buffer containing 30 mM HEPES, pH 7.4, 50 mM

[6] C. R. Vazquez de Aldana and A. G. Hinnebusch, unpublished results.

TABLE 1
Plasmids used in this study

Plasmid	Gene[a]	Selectable marker	Vector	Source
Bacterial gene fusions				
pES189-D1A	His_6[b]-*YIH1*	*Kan*^{R}	pET-28a	18
pES123-B1	*GST*[b]-*gcn1*(2052–2428)	*Am* ^{R}	pGEX-6p-3	18
pES164-2A	*GST*[b]-*gcn1*(2051–2428)-R2259A	*Am*^{R}	pGEX-6p-2	18
Yeast gene fusions				
pES245-6	*GST*[b]-*YIH1*(2–132)	*Amp*^{R}, *URA3*	pES128–9	This work
pES246-7	*GST*[b]-*YIH1*(2–171)	*Amp*^{R}, *URA3*	pES128-9	This work
pES247-8	*GST*[b]-*YIH1*(68–258)	*Amp*^{R}, *URA3*	pES128-9	This work
pES248-9	*GST*[b]-*YIH1*(68–171)	*Amp*^{R}, *URA3*	pES128-9	This work
pES249-10	*GST*[b]-*YIH1*(133–258)	*Amp*^{R}, *URA3*	pES128-9	This work
pES187-B1	*GST*[b]-*YIH1*(2–258)	*Amp*^{R}, *URA3*	pES128-9	18
pES330-5-3	*GST*[b]-*YIH1*(2–258)-E87A,D90A	*Amp*^{R}, *URA3*	pES128-9	This work
pES331-6-1	*GST*[b]-*YIH1*(2–258)-D102A,E106A	*Amp*^{R}, *URA3*	pES128-9	This work
pES332-3-1	*GST*[b]-*YIH1*(2–258)-E87A,D90A and D102A,E106A	*Amp*^{R}, *URA3*	pES128-9	This work

[a] Numbers in parentheses indicate amino acids encoded by the respective gene.
[b] Epitope tag at the N terminus of the ORF.

KCl, and 10% glycerol, was incubated for 30 min with 10 mM DTT immediately prior to protein interaction studies. The immobilized GST fusion proteins were incubated with purified His_6-Yih1 in the same buffer; the resin was extensively washed, boiled in the presence of standard 2× Laemmli SDS-PAGE loading dye, and the supernatant resolved in 10% SDS-PAGE gels. Proteins were visualized in gels by staining with Coomassie.

In Vivo GST Pulldown Assay—GST pulldown assays from yeast whole cell extract were performed as described previously (8). The precipitates were resolved by 4–12% SDS-PAGE and the proteins transferred to a PVDF membrane (Millipore). Proteins were visualized by staining the membrane with Ponceau S (0.5% (w/v), in 1% acetic acid) or by immunoblotting using antibodies for the detection of Gcn1 (HL1405, dilution 1:1000 (12)), eIF2α (1:2000 (21)), eIF2α phosphorylated on Ser-51 (1:5000; BioSource International, Inc.), Yih1 (1:1000; anti-Yih1 serum was obtained by immunization of rabbits with the His_6-Yih1 protein purified from *E. coli*, as described below), S22 (1:2000, Jan van't Riet), and actin (1:5000, (22)). Immune complexes were visualized using horseradish peroxidase conjugated to donkey anti-rabbit antibodies or to protein A (for detection of actin antibodies) (Amersham Biosciences). Protein levels were quantified using the NIH Image J software.

Molecular Modeling—MODELLER (23) was used to produce homology molecular models of Yih1. The structures of the RWD domain of Gcn2 from *Mus musculus* (Protein Data Bank code 1UKX (24)) and of the conserved hypothetical protein YigZ from *E. coli* (Protein Data Bank code 1VI7 (25)) were used as templates for constructing the model of the N-terminal domain (Yih1N, residues 1–115) and C-terminal domain (Yih1C, residues 125–258) of Yih1, respectively. These templates share marginal detectable sequence identity with their respective Yih1 domains when aligned by BLAST (26), MODELLER, THREADER (27), or CLUSTAL (28). Modeler/Clustal values for sequence identities were 17.4/19.3% for 1UKX and Yih1N and 18.9/20.0% for 1VI7 and Yih1C. The parameters used during the modeling exercise were the default of the programs. The alignments had to be inspected for correction taking into consideration secondary structure prediction and the atomic coordinates of the templates. The homology models were validated with the VERIFY-3D (29) and PROCHECK (30) softwares. The analysis was made through visualization of the superimposed structures using PyMOL (53) and various alignments produced with CLUSTAL. COOT (31) was used for the superposition (32) of the atomic coordinates of the models and Protein Data Bank files as follows: 1UKX (14) and 1VI7 (25). DALI (33), SCOP (34), CATH (35), and PFAM (36) were also used.

Recombinant Yih1 Purification and Characterization—E. coli BL21(DE3) strain (Novagen) harboring a pET28a-derived plasmid for expression of His_6-tagged Yih1, pES189-D1A, was grown in 200 ml of LB medium containing 15 μg/ml kanamycin at 37 °C until $A_{600\ nm}$ 0.2–0.4. Isopropyl 1-thio-β-D-galactopyranoside was added to a final concentration of 1 mM, and the culture was then incubated at 23 °C for 4 h. The bacterial pellet was resuspended in 1.5 ml of cold PBS containing 10 mM β-mercaptoethanol. After a cycle of freeze-thawing, lysozyme was added to a final concentration of 1 mg/ml, and after an incubation of 30 min at 37 °C, the suspension was briefly sonicated and centrifuged at 10,000 rpm (rotor SS34, Sorvall). The supernatant was applied to a column of nickel-chelating resin (Qiagen) previously washed, charged with 5 volumes of a 50 mM $NiSO_4$ solution, and equilibrated with 3 volumes of binding buffer containing 5 mM imidazole, 500 mM NaCl, 20 mM Tris-HCl, pH 8.0, and 10 mM β-mercaptoethanol. After washing with 130 volumes of binding buffer, and 30 volumes of 20 mM imidazole, 500 mM NaCl, 20 mM Tris-HCl, pH 8.0, 10 mM β-mercaptoethanol, the protein was eluted with 6 column volumes of 200 mM imidazole, 500 mM NaCl, 20 mM Tris-HCl, pH 8.0, 10 mM β-mercaptoethanol. The protein was dialyzed against 20 mM Tris-HCl, pH 8.0, 1 mM DTT, 150 mM NaCl and submitted to size exclusion FPLC on Superdex HR200 in an ÄKTA purifier system (GE Healthcare) in the same buffer, at a flow rate of 0.5 ml/min. DTT was always freshly prepared. Stokes radius and observed molecular mass of Yih1 were calculated by interpolation of the Yih1 elution volume from a plot of elution volumes of proteins with known Stokes radius/molecular mass (37). For circular dichroism analysis, far UV-CD spectra were recorded on a Jasco-810 spectropolarimeter at 20 °C using a 1 nm bandwidth and an optical path length of 0.1 mm. Ellipticity is reported as the mean residual ellipticity (θ) (degree $cm^2\ dmol^{-1}$).

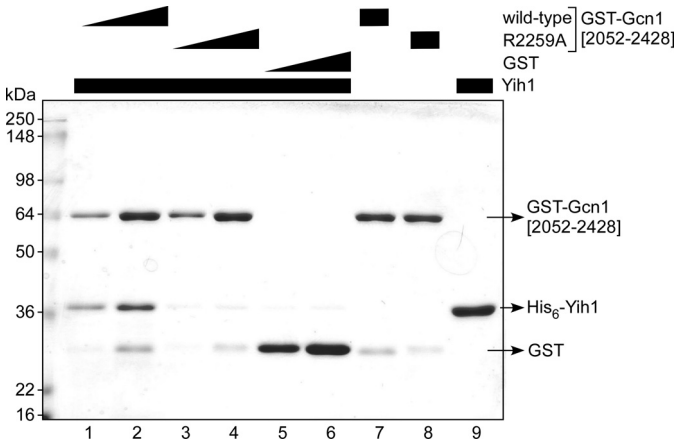

FIGURE 1. **Direct interaction between Yih1 and Gcn1, in a Gcn1-Arg-2259-dependent manner.** 2 and 4 μg of the minimal Gcn1 fragment sufficient for Yih1 binding (amino acids 2052–2428 (18)) fused to GST (GST-Gcn1(2052–2428)), the same fragment but harboring the R2259A substitution, and GST alone were overexpressed in *E. coli* and coupled to glutathione-linked affinity resin, and the bacterial proteins were removed. The beads were then incubated with 4 μg of purified His_6-tagged Yih1, and unbound proteins were washed off. The protein complex still associated to glutathione beads was then investigated via SDS-PAGE followed by Coomassie staining. As controls, 3 μg of GST fusion proteins, and 4 μg of His_6-Yih1, were loaded individually on the gel (*lanes 7–9*). In the GST-Yih1 control, *lanes 7* and *8*, a 30-kDa band putatively is GST alone resulting from degradation.

RESULTS

Yih1 and Gcn1 Directly Interact with Each Other—We have previously provided evidence suggesting that His_6-Yih1 and GST-Gcn1(2052–2428) interact directly. For this, we used GST-mediated pulldown assays and crude cell extracts of bacteria expressing the Yih1 protein and purified GST-Gcn1(2052–2428), followed by immunoblotting to detect Yih1 (18). To provide evidence for a direct interaction between these two proteins, here we employed highly purified proteins in a pulldown assay with buffer and salt compositions as used previously to show Gcn1-Gcn2 and Gcn1-Yih1 interaction (8, 18). We found that purified GST-Gcn1(2052–2428) was capable of efficiently pulling down purified His_6-Yih1 (Fig. 1, *lanes 1* and *2*). Coomassie staining of the gel used to resolve the precipitated Yih1-Gcn1 complexes showed no bands in addition to those of Yih1 or GST-Gcn1 and showed that the molar binding ratio was ~1:1. Considering that we do not know whether every GST-Gcn1 molecule interacted with Yih1, we cannot exclude the possibility that Yih1 binds to Gcn1 as a dimer or a multimer. The specificity of the interaction was verified by employing a mutant GST-Gcn1(2052–2428) fragment, where residue Arg-2259 was altered to an alanine. This mutation had been previously shown to abolish interaction with Gcn2 and Yih1 and to abolish Gcn2 activation upon amino acid starvation in yeast (8). As expected, the purified mutant protein did not co-precipitate His_6-Yih1 (Fig. 1, *lanes 3* and *4*). Taken together, these results thus clearly established that Yih1 interacts directly and specifically with a C-terminal segment of Gcn1.

Dissection of Gcn1 and Actin Binding Regions in Yih1—We have previously found that chromosomally expressed FLAG-tagged Yih1 forms a heterodimeric complex with actin monomers (G-actin) *in vivo* (18). We have shown that in GST-mediated pulldown assays overexpressed GST-Yih1 co-precipitated actin and Gcn1, but not Gcn1-R2259A, indicating that the Yih1-Gcn1 interaction in cells overexpressing Yih1 is specific and not just an artifact (18). To further understand how these interactions affect Gcn2 regulation, here we aimed to map the actin binding region in Yih1 and to compare it with the Gcn1 binding domain in Yih1. We constructed a set of various Yih1 fragments fused to GST and expressed from a plasmid with a galactose-inducible promoter (Fig. 2*A*). The expression levels of these fusion proteins were analyzed in wild-type yeast cells grown to exponential phase in medium containing galactose as a carbon source. We found that the fusion proteins were overexpressed at different levels but well above the level of the endogenous Yih1 (Fig. 2, *B–D*). To compare the amount of endogenous actin and Gcn1 sequestered in the living cell by the different GST-Yih1 fusion proteins, equal amounts of whole cell extracts were then subjected to GST pulldown assays followed by SDS-PAGE of the precipitates and immunoblotting (Fig. 3*A*). The amount of precipitated GST fusion protein was determined by Ponceau S staining of the membranes, and the amount of actin and Gcn1 co-precipitation was determined using anti-actin and anti-Gcn1 antibodies. The precipitated amounts of the different GST-Yih1 fragments correlated with their expression levels, indicating that the GST-Yih1 fragments bound to the beads with similar efficiencies. An aliquot of the inputs used in GST-pulldown assays was probed for actin and Pgk1 to ensure that in fact equal amounts of whole cell extract were used in the pulldown assay (Fig. 3*A*, *top panel*).

For quantification of the amount of Gcn1 and actin sequestered in the cell, we conducted at least three independent experiments. All experiments showed similar results to those shown in Fig. 3*A*, and the average from all results as well as the standard error were determined and used for interpretation (Fig. 3*C*). We found that overexpressed GST-Yih1(2–132), GST-Yih1(2–171), and GST-Yih1(68–258) sequestered amounts of Gcn1 approximately equal to or greater than that sequestered by the full-length fusion protein, GST-Yih1(2–258). GST-Yih1(68–171) sequestered Gcn1 weakly, possibly due to its low overexpression level. GST-Yih1(133–258), which is highly expressed, barely sequestered any Gcn1. Together, these data suggested that the Gcn1 binding region encompasses amino acids 68–132, corresponding to the C-terminal portion of the RWD domain (amino acids 4–113) (summarized in Fig. 2*A*).

To allow a semi-quantitative comparison of the Gcn1 binding affinities of the various GST-Yih1 fragments, the GST precipitation experiment was repeated as above, except that the volumes of the samples loaded on SDS-PAGE were adjusted to contain approximately the same amount of each of the precipitated GST fusion proteins (Fig. 3*B*). The amount of bound Gcn1 was then quantified relative to the precipitated amount of the respective GST-Yih1 fusion protein and presented relative to those for full-length GST-Yih1 (Fig. 3*D*). We are aware of the fact that a high expression level for a given GST-Yih1 protein may drive its interaction with Gcn1 by mass action, and we took this into account in our interpretation.

As found before, GST-Yih1(2–132), which contains only the full RWD domain, but not GST-Yih1(133–258) lacking the entire RWD domain co-precipitated Gcn1. Quantitatively, it appears that GST-Yih1(2–132) binds Gcn1 stronger than does

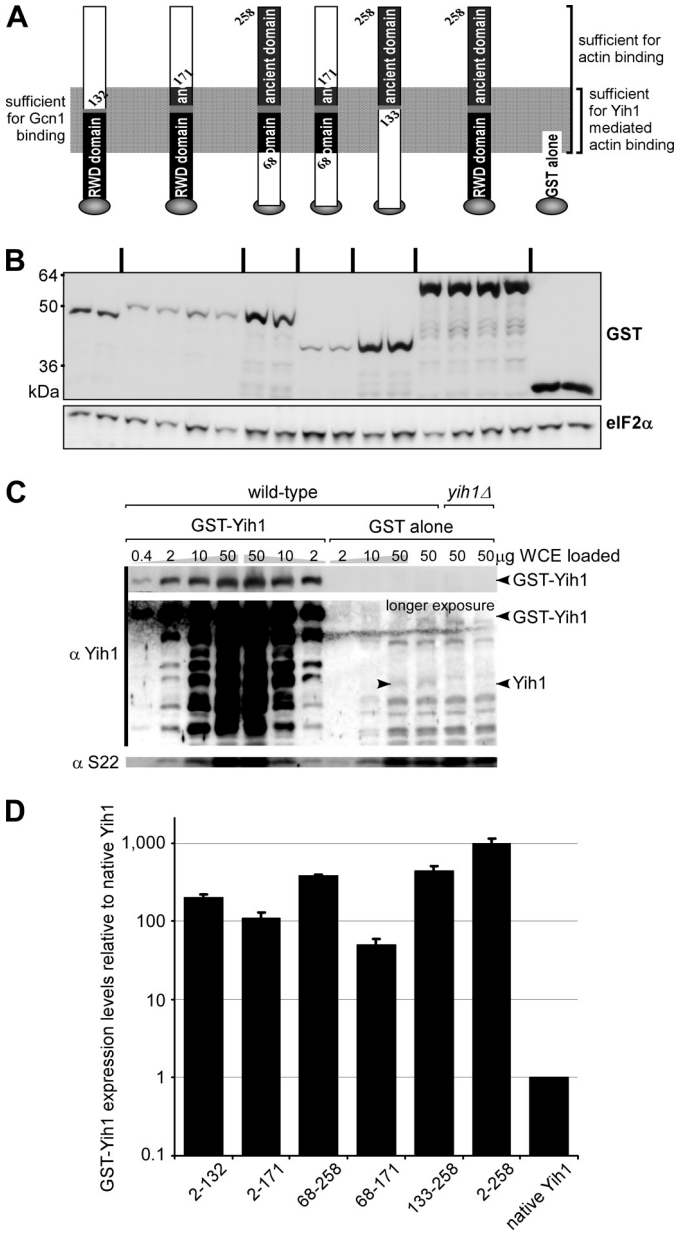

FIGURE 2. **GST-Yih1 fragments used in this study and their expression levels.** *A,* schematics of the GST-Yih1 fusion proteins harboring Yih1 fragments, including amino acids as indicated. The N-terminal RWD domain and the C-terminal ancient domain are indicated, as well as the Yih1 region sufficient for Gcn1 and actin binding and sufficient for actin binding mediated by endogenous full-length Yih1, as determined in this work. The schematic is not to scale. *B,* H1511 strains harboring plasmid-borne and GST-tagged Yih1 fragments as indicated, under a galactose-inducible promoter, were grown to exponential phase in medium containing galactose as carbon source. Equal amounts of whole cell extract was then resolved in SDS-PAGE and subjected to immunoblotting using antibodies against GST, and against eIF2α as control for equal loading. *C* and *D,* GST-Yih1 fragments are all overexpressed as compared with the endogenous Yih1. *C,* whole cell extract was generated from strain H1511 overexpressing GST-Yih1 or GST alone and from the isogenic *yih1*Δ strain ESY11001b. Various amounts of whole cell extract (*WCE*) as indicated was then subjected to immunoblotting using antibodies against Yih1, and against the small ribosomal protein S22 as loading control. For the Yih1 antibody, two different exposure times are shown. The location of GST-Yih1 and Yih1 is indicated with *arrowheads*. *D,* signal intensity from immunoblots in *B* and *C* was determined using the program NIH Image J. The Yih1 expression levels in *B* were then determined by dividing the signal intensity of the GST signal by the signal intensity of eIF2α. For *C,* the signal intensity of Yih1 found in a particular lane to be within the linear range was divided by the signal intensity of S22 found in a particular lane to be in the linear range, and then compensated for the difference in the amount of WCE loaded Yih1 signal *versus* S22 signal. Finally the signal intensities were adjusted relative to endogenous Yih1, *i.e.* the expression level of endogenous Yih1 is set to 1.

the full-length protein residues 2–258 by at least a factor of ~3 (Fig. 3*D*). Considering that GST-Yih1(2–132) is overexpressed not as strongly as residues 2–258 (Fig. 2*D*), the difference in binding strength may be even larger than it appears to be in Fig. 3, *B* and *D*. This indicates that the presence of the C-terminal portion of Yih1, containing the entire ancient domain, may hinder the interaction with Gcn1. Consistent with this, GST-Yih1(2–171), which contains only a small part of the ancient domain, also showed better binding of Gcn1 than does full-length GST-Yih1, especially considering the much lower expression level of GST-Yih1(2–171). Below it is shown that the ancient domain is required for direct binding to actin. Surprisingly, constructs GST-Yih1(68–258) and GST-Yih1(68–171), both lacking the N-terminal portion of the RWD, also appear to bind Gcn1 more strongly than does the full-length Yih1 construct (Fig. 3*D*), suggesting that the N-terminal portion of the RWD is not only dispensable but may actually hinder the interaction of Yih1 with Gcn1 *in vivo*. As shown below, however, the high level Gcn1 binding displayed by GST-Yih1(68–171) is not associated with efficient inhibition of Gcn2. Again, the construct lacking the full ancient domain (residues 68–171) seems to bind Gcn1 at higher levels than the cognate construct containing the ancient domain (residues 68–258). As summarized in Fig. 2*A*, our results show that the Yih1 minimal fragment sufficient for Gcn1 binding encompasses amino acids 68–171.

The analysis of actin co-precipitation in these same assays showed that actin associated with GST-Yih1(2–171), GST-Yih1(68–258), and GST-Yih1(68–171), but not with GST-Yih1(2–132) nor with GST-Yih1(133–258), suggesting that neither the isolated RWD domain nor the isolated ancient domain contain the complete actin binding region (summarized in Fig. 2*A*) (Fig. 3, *A* and *B*). Full-length GST-Yih1 bound actin only at very low levels that were barely above the background in these assays. Comparing the full-length construct (residues 2–258) with GST-Yih1(68–258) suggests that the presence of residues 2–67 hinders the association of actin to Yih1, similarly to their effect on Gcn1 binding.

To rule out the possibility that the binding of actin to these fragments was dependent on Gcn1, or that Gcn1 hindered actin binding to the RWD domain in Yih1, we repeated the above experiments using an isogenic strain lacking Gcn1 (*gcn1*Δ) and with equal loading of the precipitated fusion proteins (*cf.* Figs. 4*A* and 3, *B* and *D*). We found that the absence of Gcn1 did not alter the ability of these fragments to interact with actin. Thus, the interaction of Yih1 with actin does not depend on Gcn1.

We next studied whether the endogenous Yih1 present in the strain contributed to some of the interactions of GST-Yih1 fragments with Gcn1 or actin. We constructed an isogenic *yih1*Δ strain and repeated the GST-mediated co-precipitation assay. We found that Gcn1 co-precipitation did not significantly change when Yih1 was lacking in the cell (*cf.* Figs. 4*B* and 3*A*). When investigating actin co-precipitation, however, we found that although GST-Yih1(68–258) still co-precipitated

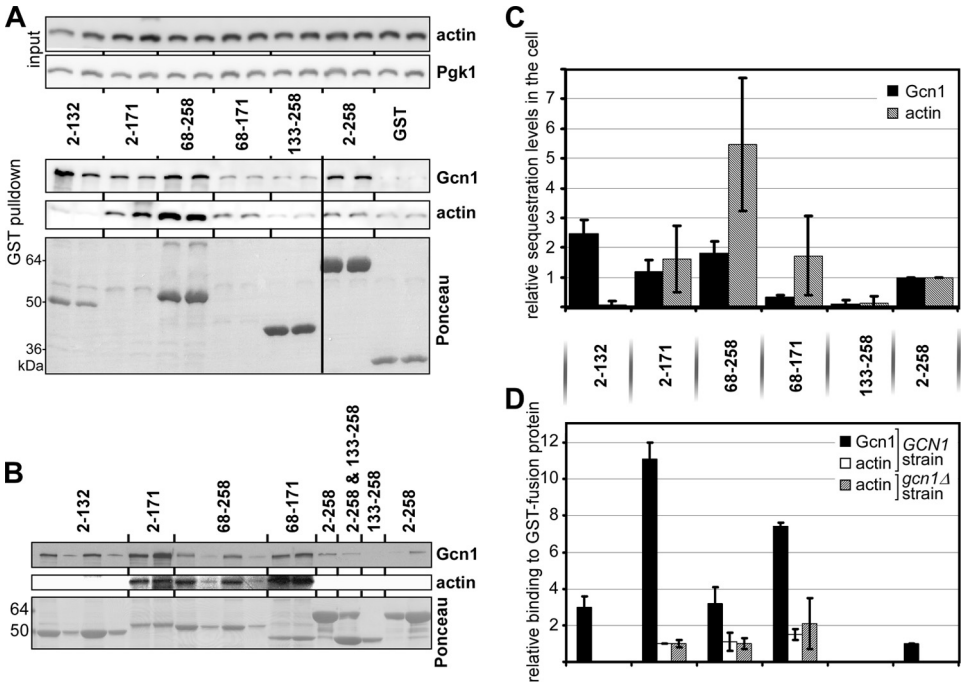

FIGURE 3. **Gcn1 and actin binding by Yih1 fragments.** *A,* identical amounts of total protein from whole cell extracts of yeast strains expressing the indicated GST-tagged Yih1 fragments were incubated with glutathione-linked affinity resin. The precipitated material was subjected to SDS-PAGE and immunoblotting using antibodies against Gcn1 and actin (*bottom panels labeled GST pulldown*). The *bottom panel* depicts the Ponceau S-stained membrane for visualization of the precipitated GST fusion proteins. For each GST fusion protein, whole cells extracts from two independent transformants were investigated. An aliquot of each sample was subjected to immunoblotting using antibodies against actin and Pgk1 to verify that equal amounts of whole extracts were used in the GST pulldown assay (*upper panels labeled input*). Three independent assays showed similar results. *B,* an identical experiment was performed as in *A,* except that the amount of the pulldown samples loaded were adjusted to normalize to the precipitated amounts of the different GST fusion proteins. Actin co-precipitation by GST-Yih1(2–258) was barely detectable due to the lower amounts of whole cell extract used as compared with *A*. *C,* amount of Gcn1 or actin sequestered in the cell in *A* was determined and normalized to the levels of full-length GST-Yih1. The standard error is indicated. *D,* amount of Gcn1 or actin bound to Yih1 fragments in *B* and Fig. 4*A* was determined by dividing the signal intensity of actin or Gcn1 by the precipitated amount of the respective GST-Yih1 fragment as determined via Ponceau S staining of the membrane (the size differences between the various GST-Yih1 fragments did not considerably affect the overall calculations (data not shown), and therefore were disregarded in the calculations). The Gcn1/Yih1 levels were normalized to that of GST-Yih1, and the actin/Yih1 levels were normalized to that of GST-Yih1(2–171) because the signal of GST-Yih1 was too weak to quantify.

actin, GST-Yih1(2–171) and Yih1(68–171) did not associate with actin in the absence of endogenous Yih1 protein (Fig. 4*B*). These last observations indicate that the association of GST-Yih1 with actin in cells lacking endogenous Yih1 requires the central region of the protein, extending from residue 68 in the RWD domain to include some or all of the ancient domain beyond residue 171.

The different results of actin binding obtained for protein 2–171 and 68–171 in the presence or absence of *YIH1* suggested that endogenous Yih1 can bridge interactions between actin and these GST-Yih1 proteins, raising the possibility that Yih1 functions as a dimer. However, a two-hybrid assay indicated that Yih1 does not interact with itself (data not shown). In addition, *in vitro*, Yih1 did not appear to form dimers (see below). It is therefore possible that Yih1 dimerizes only when bound to actin or some other unknown molecule(s). As summarized in Fig. 2*A*, the results in Figs. 3 and 4 indicate that the Gcn1 and actin-binding sites are not identical but overlap in the 68–171-residue interval.

Modulation of Gcn2 Activation by Yih1 Fragments—We next investigated whether the amounts of Gcn1 that are sequestered by the different GST-Yih1 fragments, as quantified in Fig. 3*C*, correlated with the degree of Gcn2 inhibition *in vivo*. More extensive Gcn1 sequestration by GST-Yih1 fragments should result in increased Gcn1-Gcn2 dissociation, thus reducing the level of Gcn2 activation. Gcn2 activation can be scored by growth on medium containing amino acid analogs, such as 3-amino-2,4-triazole (3AT) that causes histidine starvation. Strains unable to activate Gcn2 cannot overcome starvation and are unable to grow (Gcn^- phenotype). Overnight cultures of strains harboring plasmid-borne *GST-YIH1* alleles or GST alone as control were subjected to 10-fold serial dilutions and then transferred to solid medium containing 3AT and galactose (Fig. 5*A*). In addition, for a quantitative measure of Gcn2 inhibition, we analyzed these cells for the phosphorylation levels of eIF2α, the substrate of Gcn2. For this assay, cells overexpressing GST-Yih1 fragments, or GST alone, were grown to exponential phase and treated with 3AT before harvesting. Whole cell extracts were subjected to immunoblotting using antibodies that specifically detect phosphorylated eIF2α (eIF2α-P) and total eIF2α (Fig. 5, *C* and *D*).

As expected and published previously (9, 18), overexpressed full-length GST-Yih1(2–258) sequestered Gcn1 (Fig. 3*C*), inhibited growth on 3AT, and significantly reduced eIF2α-P levels (Fig. 5, *A, C,* and *D*). By contrast, GST-Yih1(133–258), which lacks the RWD domain, sequestered little or no Gcn1 (Fig. 3*C*) and predictably had hardly any effect on 3AT sensitivity or eIF2α-P levels (Fig. 5, *A*, *C,* and *D*). GST-Yih1(68–171), which sequestered a relatively small amount of Gcn1 (Fig. 3*C*), did not confer a Gcn^- phenotype nor a significant reduction in

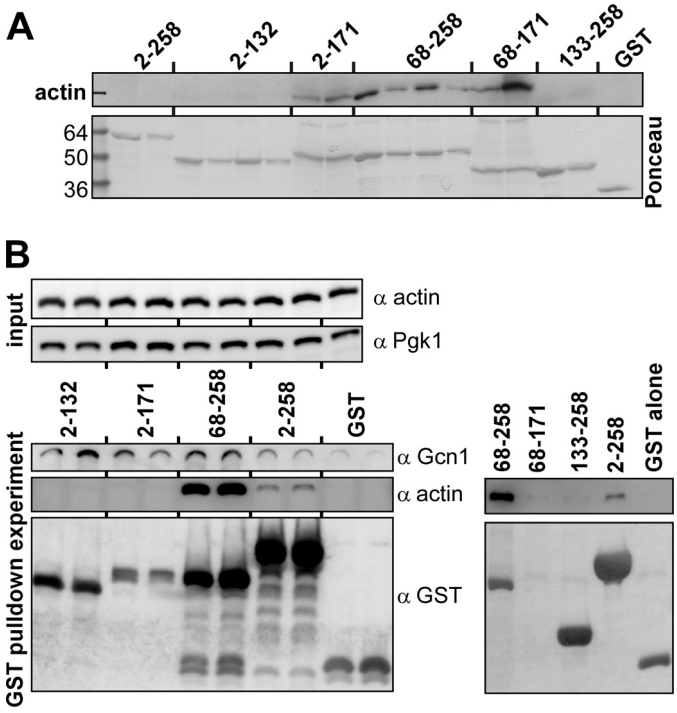

FIGURE 4. **Investigation of Yih1-actin interaction.** *A,* actin-Yih1 interaction is independent of Gcn1 *in vivo*. GST pulldown assays were performed as in Fig. 3*B* but using a strain lacking Gcn1. Actin co-precipitation by GST-Yih1(2–258) was barely detectable due to the lower amounts of whole cell extract used as compared with *B* or Fig. 3*A*. The amount of Gcn1 or actin bound to Yih1 fragments was determined in Fig. 3*D*. *B,* in Yih1 amino acids 68–258 harbor the actin binding site *per se*. GST-Yih1 fragments were investigated for their ability to co-precipitate Gcn1 or actin in a *yih1*Δ strain by conducting the same experiment as outlined in Fig. 3*A*.

eIF2α phosphorylation (Fig. 5, *A, C,* and *D*), despite its apparent high intrinsic ability to bind Gcn1 (Fig. 3*D*). This can be explained by its very low expression level (Fig. 2*D*). GST-Yih1(2–132), which sequestered a higher level of Gcn1 than did full-length Yih1 (Fig. 3*C*), consistently showed a stronger 3AT sensitivity compared with the latter (Fig. 5*A*; see also Fig. 5*B*) and reduced eIF2α phosphorylation to at least a similar extent as did full-length GST-Yih1 (Fig. 5, *A*, *C*, and *D*). GST-Yih1(2–171), which sequesters Gcn1 (Fig. 3, *A* and *C*), caused a Gcn$^-$ phenotype, albeit weaker than the full-length protein (Fig. 5,. *A, C,* and *D*). This can likely be accounted for by its low expression level (Fig. 2*D*). These findings are consistent with the expectation that the ability of Yih1 fragments to inhibit Gcn2 is generally correlated with their ability to sequester Gcn1 *in vivo*. Remarkably, however, GST-Yih1(68–258), which sequestered more Gcn1 than GST-Yih1(2–258) (Fig. 3, *A* and *C*), conferred a modest Gcn$^-$ phenotype and accordingly little inhibition of eIF2α phosphorylation (Fig. 5, *A, C,* and *D*). This last observation indicates that efficient sequestration of Gcn1 by a Yih1 fragment is not sufficient to ensure effective inhibition of Gcn2.

To investigate whether the Gcn$^-$ phenotype elicited by some of the overexpressed GST-Yih1 fragments depended on endogenous Yih1, we repeated the 3AT sensitivity (3AT^s) assay using the isogenic *yih1*Δ strain. In fact, we found that the absence of endogenous Yih1 did not substantially alter the Gcn$^-$ phenotype (Fig. 5, *A versus B*), in agreement with our findings that it does not affect the interaction of Gcn1 with any of the GST-Yih1 fragments.

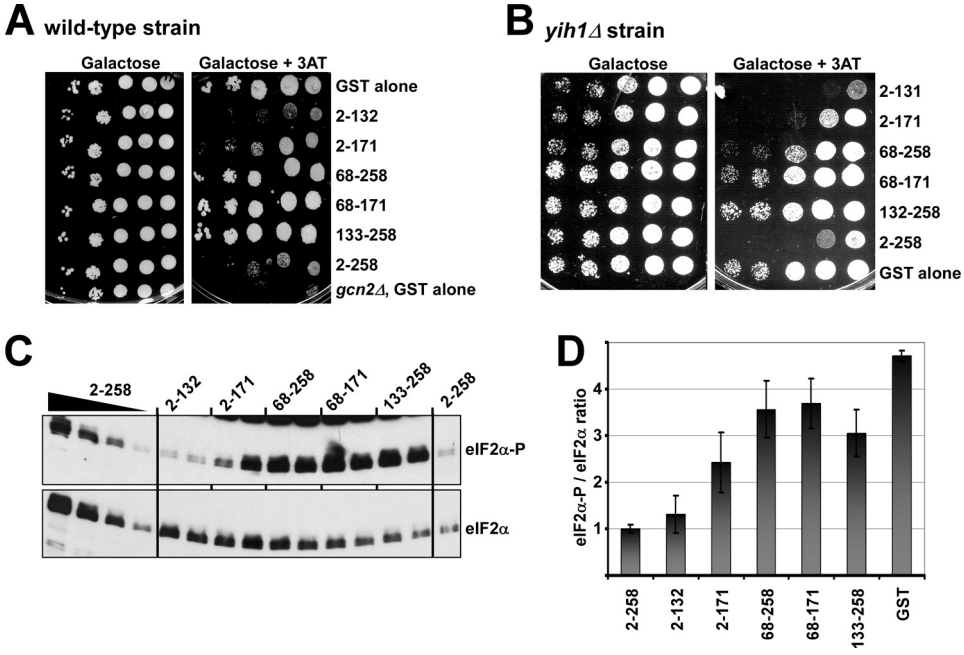

FIGURE 5. **Gcn$^-$ phenotypes associated with the overexpression of Yih1 fragments correlate with eIF2α phosphorylation levels.** *A,* 5 μl of 10-fold serial dilutions of wild-type overnight cultures expressing the indicated GST-Yih1 fusion proteins were spotted on plates containing synthetic minimal medium with galactose or galactose supplemented with 3AT. Lack of growth on medium containing 3AT is indicative of the inability to activate Gcn2 and overcome starvation (Gcn$^-$ phenotype). *B,* same assay was performed as in *A*, just that a *yih1*Δ strain was used. *C,* two independent yeast transformants harboring plasmids for the expression of GST-Yih1 fusion proteins outlined in *A* were grown to exponential phase and starved with 10 mM 3AT for 1 h before harvesting. Whole cell extracts of these cells were subjected to immunoblot analysis using antibodies against total eIF2α or phosphorylated eIF2α (*eIF2-P*). *D,* eIF2α phosphorylation in *C* was quantified relative to total eIF2α, and relative to the eIF2α/eIF2α-P level of GST-Yih1, using data from at least two independent transformants, and the standard error is indicated.

Structure-based Sequence Comparison and Modeling of Yih1 RWD Domain—The complexity of Gcn1 and actin binding to Yih1 and the resulting effects on Gcn2 inhibition, uncovered in the previous sections, together with conflicting reports in the literature regarding Gcn1-RWD domain interaction properties (9, 38) prompted us to perform comparative sequence analyses of the Yih1/IMPACT family of proteins and structural modeling to identify features that could mediate interactions with Gcn1 (Figs. 6 and 7). The RWD domain was aligned with the RWD domain of Gcn2 (Fig. 6*A*). The structural features of the RWD domain of mouse Gcn2 (Protein Data Bank code 1UKX), as determined by NMR (14), are indicated at the bottom of the alignment. As published previously, the RWD domain shows little sequence conservation, both within the Yih1/IMPACT family and the Gcn2 family of proteins, except for a few residues that are identical in all proteins, as highlighted in the alignment (Fig. 6*A*) (9, 14). Our modeling of Yih1(1–115) on the 1UKX structure of the mouse Gcn2 indicated that it can conform to the α-β two-layer sandwich of one β-sheet (four β-strands) and three α-helices (Fig. 6*A*). From the NMR structures of 1UKX, it is possible to notice that the regions of greater movement are located between strands B1 and B2 and between B2 and B3. In Yih1, and also from the sequence of its orthologs, these regions are shorter than in Gcn2 and should be less flexible. In the motif P*XX*YP*XXX*P, between strands B3 and B4, that forms a characteristic triple β-turn found only in the RWD, UBC, and UEV classes of proteins, the Yih1/IMPACT family includes an additional Pro that is completely invariant (P*XX*YP*XXX*PP) suggesting a more rigid conformation in the triple β-turn. This motif is an essential structural determinant, forming an internal hydrogen bond network, and mutations of the YP residues in Gcn2 were shown to cause improper folding and loss of secondary structure (14). The invariant residues in this motif contact the invariant Gly residue located in the loop between helices H2 and H3 (indicated in Fig. 7*A*) and residues in the beginning of H3. Another important conformational determinant is the invariant Glu in helix H1 that contacts the first two residues of helix H3 (Met and Ile in mouse Gcn2). In our modeling, all these relevant contacts are preserved in Yih1, as indicated by the *dotted lines* in Fig. 7*A*, confirming that the RWD domain of Yih1 is structurally similar to that of Gcn2.

Our deletion analysis clearly indicated that Yih1 amino acids 2–132 are sufficient for Gcn1 binding, although amino acids 68–171 and 68–258 can also bind Gcn1 (Fig. 3), suggesting that within the RWD domain the helices H2 and H3, between amino acids 74 and 114 at the C-terminal end of the RWD domain, encompass the main determinants for Gcn1 binding. This is in agreement with the fact that H2 and H3 are positioned close to each other on the same Yih1 surface, although H1 faces a different side of the protein, and thus a simultaneous interaction of Gcn1 with H1, H2, and H3 seems unlikely. The 50% decrease in GST-Yih1(68–171) expression relative to GST-Yih1(2–171) (Fig. 2*B*) may suggest protein instability due to the lack of H1.

Yih1 Amino Acids Asp-102 and Glu-106 Are Required for Gcn1 Binding—Gcn2 residues Glu-125, and Glu-136 in H3, have been proposed to contact Gcn1 based on their conservation, solvent accessibility, and charge given the relevance of the Arg-2259 residue of Gcn1 in the binding to Gcn2 (8, 14). This same Gcn1 residue was shown here to be fundamental in mediating the direct interaction with Yih1 (Fig. 1). Thus, we analyzed the Yih1 model for similar contacts (Fig. 7*A*). In our Yih1 model, Yih1 residue Asp-102 in H3 occupies the same position in the helix as Glu-125 in Gcn2, with the side chain exposed to the solvent. Yih1 does not have a similarly charged residue as Gcn2 Glu-136 in H3; however, the Yih1 Glu-106 side chain is exposed on the surface in H3. In helix H2, Yih1 Glu-87 and Gcn2 Glu-117 are found in the same position, with their side chains on the surface of the molecule. In addition, Yih1 contains another acidic residue in H2, Asp-90, that could be involved in contacting Gcn1. We then wanted to test whether these amino acids are necessary for Gcn1-Yih1 interaction. We substituted in GST-Yih1 amino acids Glu-87 and Asp-90 in helix 2, Asp-102 and Glu-106 in helix 3, and all four amino acids by alanines. The resulting mutant gene constructs (named *GST-YIH1*H2*, *GST-YIH1*H3*, and *GST-YIH1*H2*H3*), and wild-type *GST-YIH1* and *GST* alone as control, were introduced into the wild-type strain H1511 or its isogenic *yih1*Δ strain ESY11001b. To investigate whether the amino acid substitutions abolish the ability of GST-Yih1 to bind Gcn1 and inhibit Gcn2 activation, we subjected the transformants to 3AT^s assays and GST-mediated pulldown assays as outlined above. Importantly, in both the *YIH1*$^+$ and *yih1*Δ strain, we found that overexpressed GST-Yih1*H3 was unable to inhibit Gcn2 activation as determined by the inability of the cells to grow on 3AT (Fig. 8, *A* and *B*). This effect correlated with a significant reduction in Gcn1 co-precipitation but not in actin co-precipitation (Fig. 8*C*), strongly suggesting that Asp-102 and Glu-106 are involved in contacting Gcn1.

GST-Yih1*H2, on the other hand, was able to elicit sensitivity to 3AT, indicative of a strong inhibition of Gcn2 (Fig. 8, *A* and *B*). In fact its phenotype was slightly stronger than that caused by GST-Yih1 even though their expression levels were similar (Fig. 8*C*, *top panel*). This stronger Gcn$^-$ phenotype correlated with GST-Yih1*H2 co-precipitating slightly more Gcn1 than GST-Yih1 (Fig. 8*C, bottom panel*). Curiously, GST-Yih1*H2 also co-precipitated far more actin than GST-Yih1, suggesting that the E87A,D90A substitutions may have relaxed the Yih1 structure such that actin and Gcn1 have better access to their binding sites.

Next, we investigated the effects on Yih1 when mutations in both helices were combined. Overexpression of GST-Yih1*H2*H3 did not lead to a Gcn$^-$ phenotype, and this correlated with a reduction in Gcn1 sequestration. However, GST-Yih1*H2*H3 still sequestered more actin than GST-Yih1.

Taken together, our studies suggest that Asp-102 and E106A in Yih1 helix 3 are involved in contacting Gcn1 and that Glu-87 and Asp-90 in helix 2 contribute in restricting access of Gcn1 and actin to their binding sites in Yih1.

Structure-based Sequence Comparison and Modeling of the YIH1 Ancient Domain—We compared the ancient domain segment of Yih1 and its orthologs with the UPF0029 motif of the YigZ family of prokaryotic proteins (Fig. 6*B*). The structural features of the UPF0029 domain of YigZ (Protein Data Bank code 1VI7), determined by crystallography (25), are indicated at the bottom of the alignment. This alignment also includes

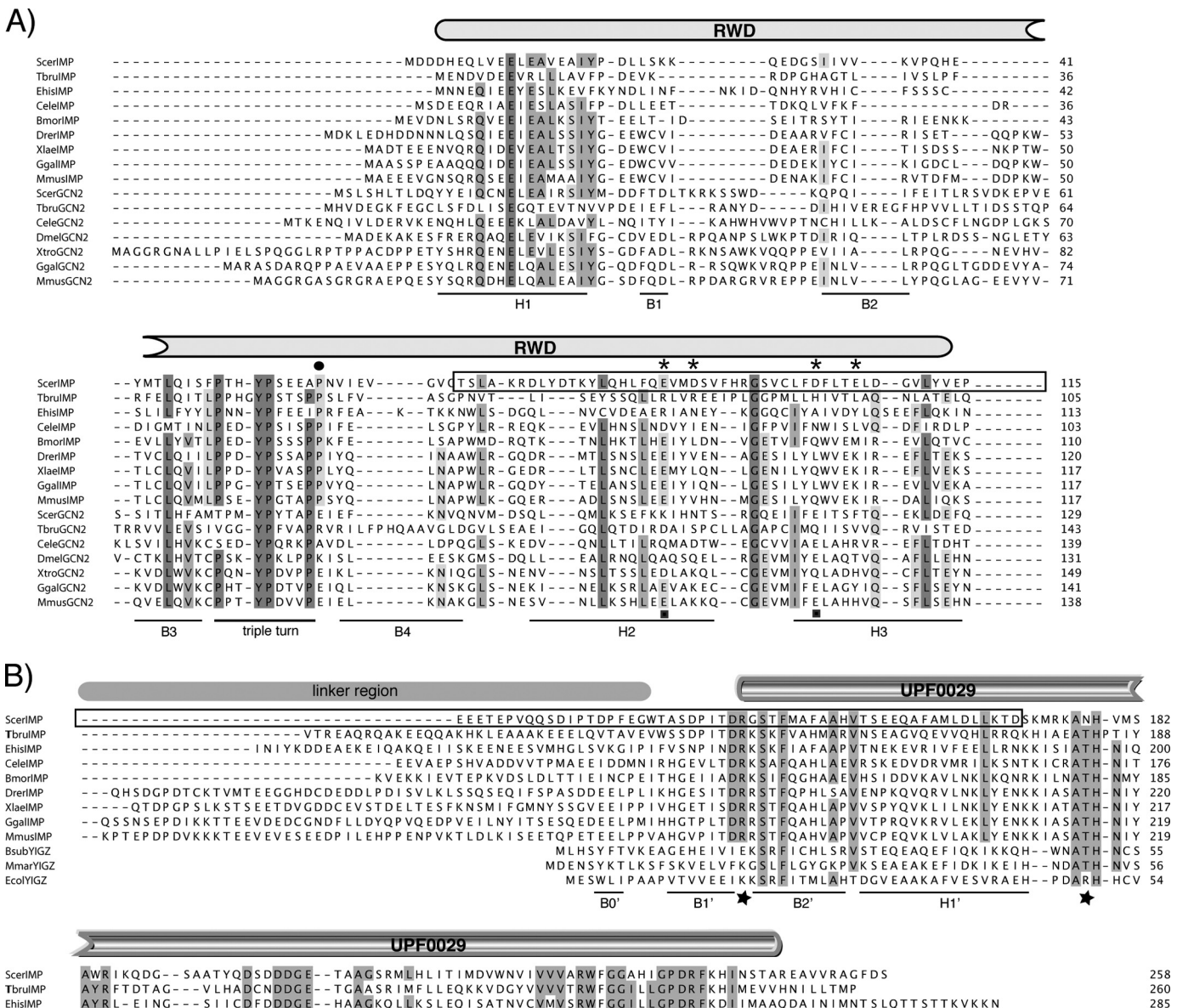

FIGURE 6. **Sequence alignment of the Yih1/IMPACT family of proteins.** The proteins of organisms from diverse phylogenetic groups are shown in the alignments, with identical residues *highlighted*. The structural features of the *M. musculus* Gcn2 RWD domain and of the *E. coli* YigZ protein are shown at the *bottom* of the respective alignments. *A,* alignment of the RWD domain of Yih1/IMPACT and Gcn2. The *black dot* at the *top* of the alignment indicates the invariant proline found in the Yih1/IMPACT family of proteins at the triple β-turn. The *black squares below* the alignment in helices H2 and H3 indicate the positions of putative Gcn1 contacts that are conserved in Gcn2 and Yih1, as suggested by the modeling studies based on the Gcn2 structure (14). The *asterisks above* the yeast sequence in helices H2 and H3 of the RWD domain indicate the residues that were mutated to alanine in this work. *B,* alignment of the UPF0029 domain of Yih1/IMPACT with the corresponding domain of prokaryotic proteins. The minimal region in Yih1 sufficient for the binding of Gcn1 is indicated by a *box* encompassing *A* and *B*. The *stars* at the *bottom* of the alignment indicate the loops that face the same position in the structural model. *S. cerevisiae* (*Scer*) (Yih1-gi:6319904; Gcn2-gi:6320489); protozoan *Trypanosoma brucei* (*Tbru*) (IMPACT-gi:74025192); nematode *Caenorhabditis elegans* (*Cele*) (IMPACT-gi:71995232; Gcn2-gi:17537697); silk worm *Bombyx mori* (*Bmor*) (IMPACT-gi:148298701); zebrafish *Danio rerio* (*Drer*) (IMPACT-gi:53933252); frog *Xenopus laevis* (*Xlae*) (IMPACT-gi:82119738; Gcn2-gi:24082513); bird *Gallus gallus* (*Ggal*) (IMPACT-gi:118086906; Gcn2-gi:118091755); *M. musculus* (*Mmus*) (IMPACT-gi:6680447; Gcn2 gi:166851838); Gram-negative bacterium *E. coli* (gi:14917068); Gram-positive bacterium *Bacillus subtilis* (gi:3123311), and the archaea *Methanococcus maripaludis* (Q6LYD0).

sequences in the Yih1 family of proteins that separate this domain from the RWD domain and that are not found in the prokaryotic family. This segment is dubbed in this work as the Linker Region, which is longer in the vertebrate lineage (Fig. 6*B*). It has no obvious sequence conservation except for the abundance of charged residues, especially evident in higher

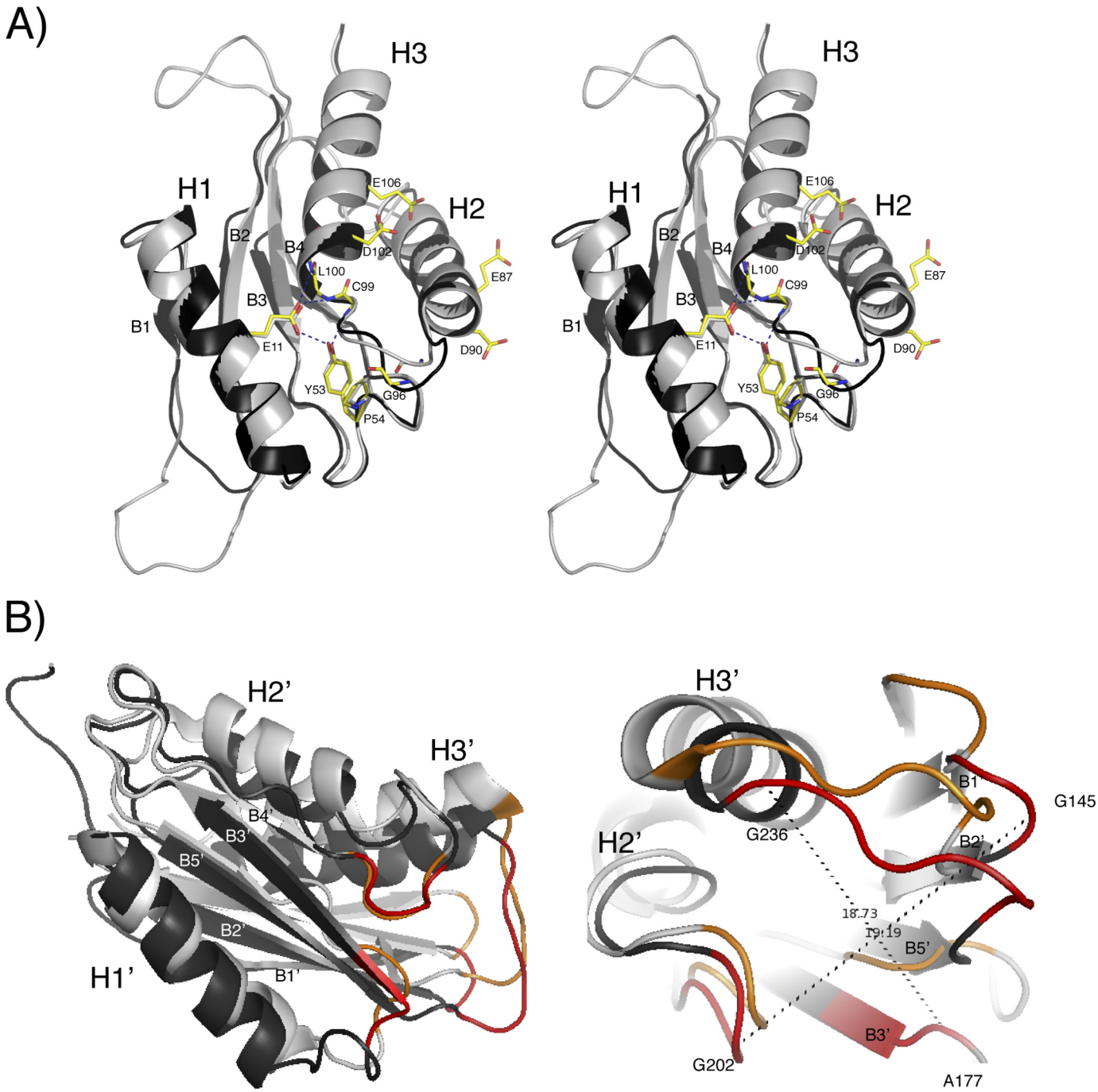

FIGURE 7. **Modeling of Yih1.** Schematic of the models for the Yih1 RWD domain, in stereo view (*A*) and the UPF2009 domain, also called the ancient domain (*B*), are shown in *black*. The structures of Gcn2 RWD and of YigZ UPF0029 domains are superimposed in *gray* in the respective schematics. *A*, side chains of amino acid residues E, in helix H1, YP, in the triple β-turn, and G, between H2 and H3, are shown in *sticks* superimposed for Yih1 and for Gcn2. The hydrogen bonds between E and Y and with the three first residues in H3 are indicated. The surface-exposed side chains of acidic residues in Yih1 H2 (Glu-87 and Asp-90) and H3 (Asp-102 and Glu-106) are indicated as *sticks*. *B*, features shown in *red* are of the Yih1 protein and those in *orange* are of YigZ. The schematic shown in the *right panel* in *B* corresponds to a head-on view of the loops with conserved residues, identifiable by the indicated residues of each loop. The distances in Å are shown by the *dotted lines*.

eukaryotes, suggesting that it does not form a tightly packed domain. Supporting this idea, prediction algorithms, such as Disopred and FoldIndex, indicated that the linker segment in Yih1 and in its orthologs is an unstructured region of the protein (data not shown). In the UPF0029 domain, the sequence similarity among the eukaryotic and prokaryotic proteins is restricted to several highly conserved residues (Fig. 6*B*).

Yih1(125–258) was then modeled based on the 1VI7 structure of the *E. coli* YigZ protein (Fig. 7*B*) (25). 1Vl7 has a unique fold and consists of an α-β three-layer sandwich of one α-helix on one side, a five-stranded β-sheet in the middle, and two α-helices on the other side (Fig. 7*B*). Except for B0′, all other structural features of YigZ accommodated the Yih1 sequences (Fig. 7*B*).

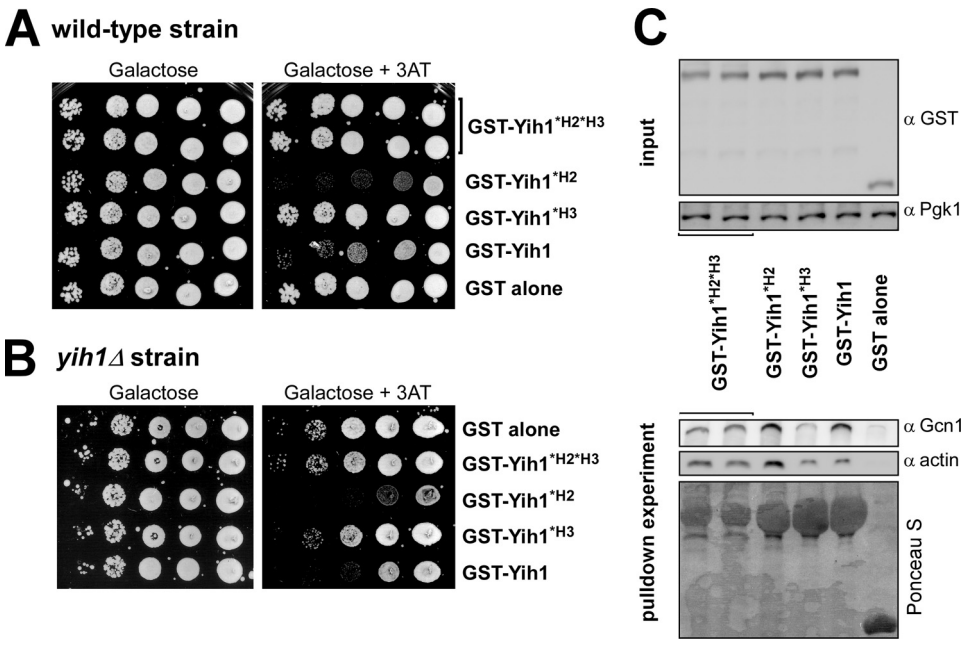

FIGURE 8. **Effect of Yih1 RWD domain amino acid substitutions on Gcn2 activation and Gcn1 binding.** Wild-type strains (*A*) and *yih1*Δ strains (*B*) harboring GST-Yih1 fusion proteins as indicated were subjected to Gcn$^-$ phenotype assays as outlined in Fig. 5. GST-Yih1 depicts the Yih1 wild-type version, although *H2 depicts E87A,D90A substitutions, and *H3 D102A,E106A depicts substitutions in RWD domain helix 2 and 3, respectively. *C,* expression level of the GST-Yih1 fusion proteins (*top panel*) and their ability to sequester Gcn1 and actin (*bottom panel*) were determined as outlined in Fig. 3*A*.

Despite its high conservation, the function of the UPF0029 domain is not known, and YigZ as well as Yih1 are nonessential proteins under normal growth conditions. Because of the lack of functional information on this domain in other proteins, we decided to analyze in more detail our modeling exercise. We found that several highly conserved features are signatures of either the eukaryotic or the prokaryotic proteins. Of particular interest are the absolutely conserved DDGE motif, between B4′ and H2′, which is followed by an invariant proline in all prokaryotes, but not in eukaryotes, and amino acid motifs in the beginning of H3′ that clearly distinguish the eukaryotic from the prokaryotic proteins. In the latter case, eukaryotes show the motif GPDRF(R/K)*X*L*X*, whereas prokaryotes show the motif G*X*GGL*X*(R/K)AY (Fig. 6*B*). Interestingly, the highly conserved sequence features are found in loop regions (between B1′ and B2′, H1′ and B3′, B4′ and H2′, and B5′ and H3′) and are located on the same side of the molecule, in both Yih1 and YigZ, as shown in *red* and *orange* colors in Fig. 7*B*. These loops form a surface of about 19 Å at its largest dimensions (Fig. 7*B*, *right panel*), suggesting that these conserved motifs may be involved in the binding of a molecule/protein that is evolutionarily conserved among eukaryotes and prokaryotes. The eukaryotic and prokaryotic determinants we found next to the DDGE motif in the loop between B4′ and H2′, and the eukaryotic PDRF or the prokaryotic GGL motifs in the beginning of H3′, may reflect peculiarities of their respective putative binding partners.

Conformational Analysis of Full-length Yih1—Our sequence conservation analysis and modeling studies suggested that Yih1 may consist of two domains connected by an unstructured linker region. However, our data on Gcn1 and actin binding suggested that overlapping elements encompassing both domains contribute to these interactions. Thus, to provide additional information to support our predictions, we performed an initial characterization of the overall conformation of Yih1 by analyzing purified recombinant His_6-Yih1 by size exclusion chromatography on a Superdex HR200 column. Molecular size standards (BSA and GST) were applied to the same column for calibration. As shown in Fig. 9*A*, Yih1 elutes as a sharp peak at around 48 kDa, larger than the theoretical predicted value of 31.8 kDa. From the elution behavior of Yih1 compared with the indicated standards, the Stokes radius was calculated to be 28.7 Å, similar to that of a globular 43.3-kDa protein. Because of the larger than expected size, we next proceeded to determine whether the peak eluting at 48 kDa could represent a dimer. Although structural data suggest that neither the Gcn2 RWD domain nor YigZ form dimers (14, 25), the presence of the charged linker region could be mediating electrostatic intermolecular interactions. We therefore performed size exclusion chromatography in the presence of the chaotropic agent potassium iodide. No evidence of a smaller protein peak that could represent a monomer was obtained using 0.5 M or even 1 M KI, although part of the protein eluted with a larger heterogeneous size indicative of denaturation (data not shown), suggesting that purified Yih1 is probably monomeric, at least under our experimental conditions, and is not a tight globular protein. These results, together with two-hybrid assays (data not shown), indicate that Yih1 probably does not dimerize. CD analysis of the purified His_6-Yih1 protein indicated that it has a proper folding (Fig. 9*B*). Based on the CD spectrum, we calculated that the protein is composed of 28.9% helices, 23.7% β-sheets, 19.5% turns, and 27.9% random structure, values that are within the range obtained in our modeling exercise (39). Our results suggest then that the RWD domain and ancient domain are well structured. The observation that in size exclusion chromatography Yih1 migrates as a larger protein than expected indicated that Yih1 is not a tight globular protein.

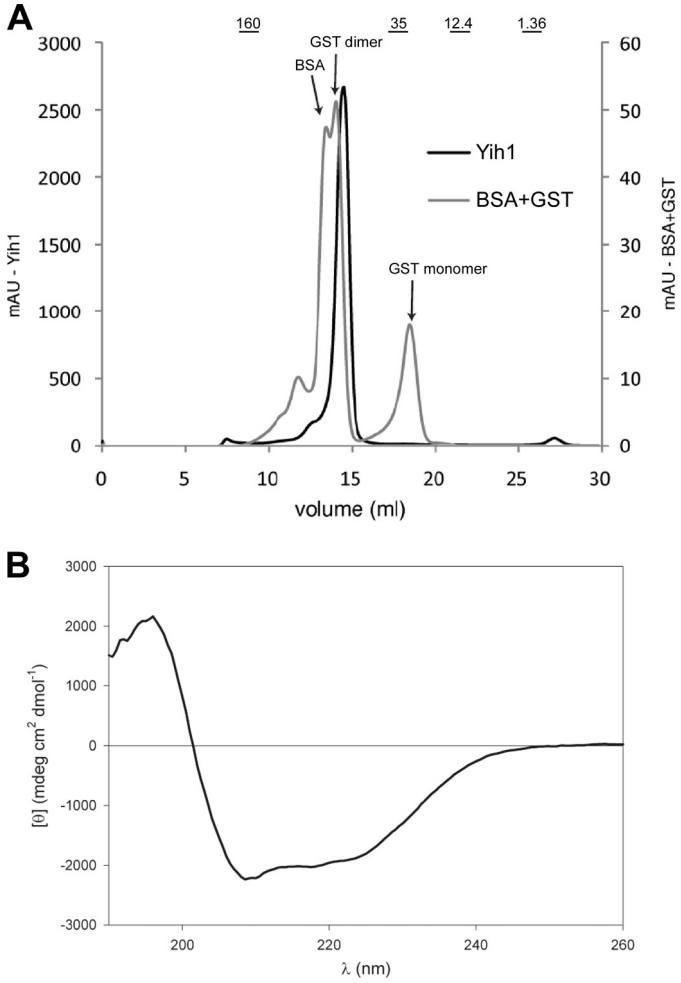

FIGURE 9. **Yih1 conformational analysis.** *A,* size exclusion chromatography on Superdex HR200 (0.5 ml/min) of the nickel-affinity resin purified His_6-Yih1 protein (1.8 mg) (*left axis*) and of BSA (67 kDa) and GST (27 kDa) (100 μg each) (*right axis*) in 20 mM Tris, pH 8.0, 1 mM DTT, and 150 mM NaCl. At the *top* of the *graph*, the *bars* indicate the elution positions of proteins of the following mass: 160 kDa, bovine gamma globulin; 35 kDa, β-lactoglobulin; 12.4 kDa, cytochrome *c,* and 1.36 kDa, vitamin B_{12}. Stokes radius (R_S) is as follows: bovine gamma globulin: R_S, 48 Å; BSA, R_S, 35.5 Å; cytochrome *c,* 17 Å. *B,* circular dichroism spectrum of His_6-Yih1.

Taken together, our data suggest that the two domains are structurally largely independent of each other with the linker region providing an unstructured and flexible region. This, however, does not exclude the possibility that the domains influence each other functionally.

DISCUSSION

In this study, we have obtained new insights into the mechanism of the Yih1-mediated regulation of Gcn2. Here, we demonstrated that *in vitro* Yih1 directly binds to Gcn1, and thus independently of actin, and that *in vivo* Yih1 can bind Gcn1 and actin independently of each other, supporting our model that Yih1 shuttles between its binding partners Gcn1 and actin. Importantly, we discovered that Gcn1- and actin-binding sites in Yih1 overlap, and we obtained evidence that actin binding to Yih1 may indeed modulate its ability to bind Gcn1 and inhibit Gcn2. We also discovered that not all Yih1 proteins able to bind Gcn1 *in vivo* can inhibit Gcn2, as an intact RWD domain is required for Gcn2 inhibition even though efficient Gcn1 binding can be achieved with only the C-terminal portion of the RWD.

We have shown here that residues 2–132 of Yih1 bind Gcn1 in yeast cell extracts and inhibit Gcn2 activation *in vivo*, thus defining the RWD domain as sufficient for these activities. Our data are in agreement with previous reports that polypeptide fragments containing residues 1–125 of Yih1 and 1–125 of Gcn2 were capable of binding Gcn1 and of inhibiting Gcn2 (9, 38). Importantly, our results also indicated that residues 1–67 are dispensable for Yih1 to bind Gcn1, suggesting that helices 2 and 3 of the RWD domain mediate this interaction. However, Kubota *et al.* (9) reported that a Gcn2 fragment comprising residues 28–125 and comprising H2 and H3 did not interact with Gcn1 in two-hybrid assays in yeast. Moreover, mutations in the YP*XXX*P motif of the triple β-turn of yeast Gcn2 RWD domain were also described to completely abolish the binding to Gcn1, as determined by two-hybrid analysis and *in vitro* overlay assays, and it was reported as "data not shown" that mutations in YP*XXX*P of Yih1 had the same effect (9). These reports seem to be incompatible with our data by suggesting that Yih1 residues N-terminal to H2-H3 are critical for Gcn1 binding. One explanation for the conflicting results is that the proteins mutated in YP*XXX*P or lacking H1 were not stably expressed in the cells. Supporting this idea, mutations in the YP residues of mammalian Gcn2 result in loss of structure of the protein (14), and mutations in the YP residues of IMPACT abolish its stable expression in mammalian cells.[7] In fact, those authors (9) did not provide evidence that the Gcn2 RWD fragments harboring YP*XXX*P substitutions or lacking helix H1 were stably expressed in cells.

Through structural modeling followed by mutagenesis, we succeeded in showing that surface-exposed acidic residues located in helix H3 (Asp-102 and Glu-106) are essential for Gcn1 binding *in vivo*, thus adding support to our deletion mapping analysis. These results also bear relevance for Gcn2 function, because the corresponding residues in H3 of Gcn2 RWD domain should contact Gcn1 and thus be essential for Gcn2 activation. Interestingly, Ala substitutions of Glu-87 and Asp-90 in H2 lead to increased Gcn1 sequestration. Considering that these amino acids are predicted to be solvent-exposed, their charge may restrict access to Gcn1, and the Ala substitutions would thus facilitate better access of Gcn1 to its binding site on H3.

Our deletion studies also showed that actin binding to Yih1 requires part of the RWD that was shown to bind Gcn1, in addition to most if not all of the ancient domain. The fact that the mutations in H3 affected Gcn1 but not actin binding strongly suggested that in RWD the binding determinants for Gcn1 and actin are different. Importantly, the results of the mutations in H2, which increased both actin and Gcn1 binding, suggest that these molecules occupy a spatially contiguous surface on Yih1 RWD. Also supporting this view, the N-terminal region comprising residues 2–68 constrains access of both actin and Gcn1 to Yih1, probably by maintaining a tight conformation of helix H2 relative to helix H3, as indicated by the

[7] C. M. Pereira and B. A. Castilho, unpublished data.

intramolecular contacts in our modeling studies. Thus, actin and Gcn1 binding seems to involve different but partially overlapping regions of Yih1. An exclusive interaction with each of these partners may explain our observation that the RWD domain alone (residues 2–132), which does not interact with actin, binds Gcn1 more efficiently. Based on the most sensitive assay for Gcn2 function *in vivo*, 3AT-resistance, construct 2–132 is also a stronger Gcn2 inhibitor than is full-length Yih1.

Our analysis provided evidence that the efficiency of a Yih1 fragment in sequestering Gcn1 does not necessarily dictate its ability to inhibit Gcn2 activation. Notably, GST-Yih1(68–258) sequesters more Gcn1 than does full-length GST-Yih1 but is quite inefficient at inhibiting Gcn2 function. To properly interpret the Gcn$^-$ phenotypes elicited by the constructs that bind Gcn1 efficiently, it should be noted that several lines of evidence indicate that there is a pool of Gcn1 not engaged in contacting Gcn2 as follows: (i) various polysome co-sedimentation assays indicate that only about 50% of Gcn1 resides on the ribosome (8, 10, 13); (ii) there are 26 times more Gcn1 molecules than Gcn2 in the cell (40); and (iii) several comprehensive protein-protein interaction studies showed that Gcn1 is in several complexes lacking Gcn2 (41, 42). Thus, certain Yih1 deletions or mutants, although still capable of efficiently binding to Gcn1, may not be able to displace pre-formed Gcn1-Gcn2 complexes (Fig. 10*B*). Thus, a likely interpretation for the inability of protein 68–258 to inhibit Gcn2 is that the lack of H1 and of the YP*XXX*P motif, both necessary to stabilize the conformation of H2 relative to H3, would impede the displacement of Gcn1 from an already formed Gcn1-Gcn2 complex and instead lead to binding to those Gcn1 molecules that are not interacting with Gcn2. Because the 68–258-residue construct actually binds Gcn1 more efficiently than does full-length Yih1, it seems necessary to also propose that destabilizing the H2-H3 portion of the RWD somehow increases the ability of Yih1 to interact with Gcn1 molecules in cellular locations or to engage in complexes with other molecules that do not participate in regulating Gcn2, while decreasing its ability to compete with Gcn2 and displace Gcn1 from Gcn1-Gcn2 complexes. The destabilization of H2 and H3 conformation by removing residues 1–67 also results in stronger actin binding. Interestingly, the full-length *H2 mutant binds both Gcn1 and actin stronger than the wild-type Yih1, and yet it is a much stronger inhibitor of Gcn2 when compared with the latter. A likely scenario in this case is that the negative effect of increased actin binding preventing Gcn1-Gcn2 destabilization would be counterbalanced by the largely increased affinity of Yih1*H2 to Gcn1. Thus, the Yih1*H2 molecules not bound to actin would displace the Gcn1-Gcn2 complex with higher efficiency than the wild-type protein.

GST-Yih1(2–171) is a good inhibitor of Gcn2, especially considering its lower expression level and thus its ability to sequester Gcn1 when compared with protein 2–171. Considering that protein 2–171 harbors the complete RWD domain and is incapable of binding actin, this agrees with our idea that actin negatively affects Yih1-Gcn1 binding. Regarding protein GST-Yih1(68–171), it is difficult to address quantitatively its ability to inhibit Gcn2, given its extremely low expression levels.

Based on our deletion and mutational data, we propose then that the binding of actin to the segment 68–258 would (partially) mask the Gcn1-binding site (Fig. 10) and that segment 1–67 is required to efficiently disrupt Gcn1-Gcn2 interaction (Fig. 10*B*). Our data indicated that the RWD and ancient domains are well structured and connected via an unstructured and flexible linker region. These domains then may adopt dif-

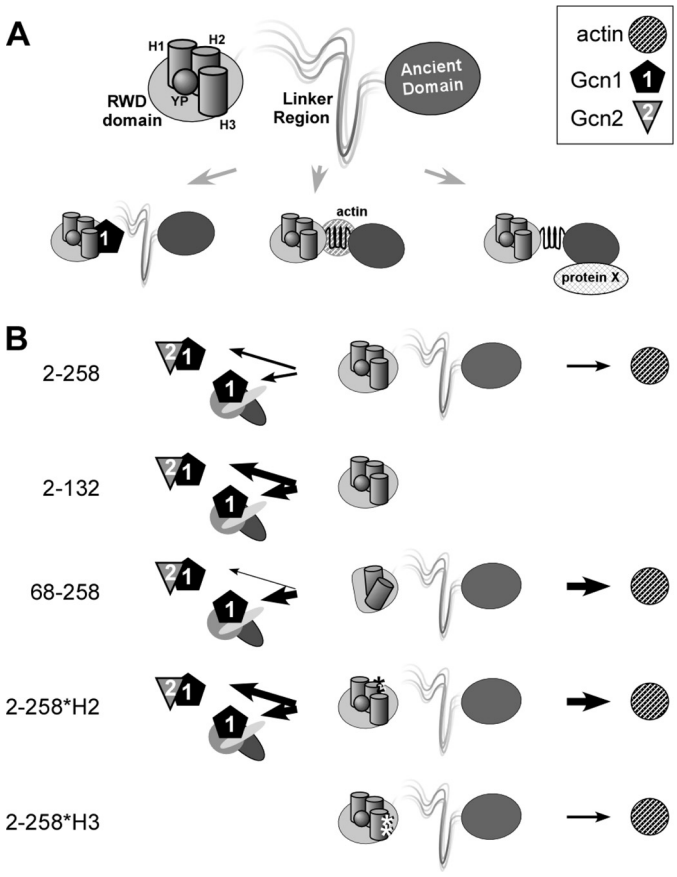

FIGURE 10. **Model for Yih1 function.** *A,* based on our findings, we propose that the Yih1 RWD domain and the ancient domain are linked by an unstructured and flexible linker region. Yih1 binds Gcn1 (*left arrow*) or actin (*middle arrow*). We cannot exclude the possibility that Yih1 binds actin and Gcn1 simultaneously. We propose that Yih1-actin interaction prevents Yih1 from efficiently sequestering Gcn1 from Gcn2, and thus from efficiently inhibiting Gcn2 activation. We have pinpointed a region common to all Yih1/IMPACT ancient domains that may bind other factors or proteins, here dubbed protein X (*right arrow*). RWD domain helices H1, H2, and H3 are shown as *cylinders*, and the invariant YP*XXX*P motif is shown as a *ball* labeled with YP. *B,* models for various Yih1 proteins, as indicated on the *left* by the amino acid numbers, and mutations in Helix 2 or 3 as indicated as **H2* or **H3*. The *thickness of arrows* indicates the relative preference of interaction. *2–258*, wild-type Yih1 may form different complexes in cells. One complex, solely dependent on the RWD domain, is formed with Gcn1. Yih1 may either compete with Gcn2 for Gcn1 binding or bind Gcn1 engaged in complexes with other molecules that do not participate in regulating Gcn2. Another complex is formed with actin and depends on part of the RWD domain, the linker region, and part, if not all, of the ancient domain. *2–132,* RWD domain on its own has the same properties as full-length Yih1, just that it cannot bind actin (protein 2–171, not included in this schematics seems to behave similarly). *68–258*, lack of amino acids 2–67 increases the binding to Gcn1 and actin but renders Yih1 incapable of inhibiting Gcn2, suggesting that a complete RWD domain is required for disrupting Gcn1-Gcn2 interaction or for sustaining a Yih1-Gcn1 interaction in presence of Gcn2. *2–258*H2,* amino acid substitutions E87A,D90A in RWD domain helix 2 (indicated as **) allow better access of Gcn1 and actin to their binding sites in Yih1. Because of the presence of a complete RWD domain, this protein is able to efficiently bind to Gcn1 complexed or not with Gcn2. *2–258*H3,* amino acids Asp-102 and Glu-106 in helix 3 are essential for Gcn1 binding, and when mutated (as indicated as **) affect Gcn1 binding but not actin binding.

ferent conformations in the cell according to their binding partner, actin or Gcn1.

Curiously, we observed that GST-Yih1(2–171) and GST-Yih1(68–171) mediated strong actin co-precipitation only when the endogenous Yih1 was present in the cell, suggesting that a full-length Yih1 bridged this interaction. Even though our biochemical studies consistently indicated that Yih1 does not dimerize or oligomerize, we cannot exclude the possibility that Yih1 dimerizes *in vivo*. Considering that GST-Yih1(2–132) does not precipitate actin even in the presence of endogenous Yih1, the component responsible for actin interaction in the presence of endogenous Yih1 must include amino acids 133–171. Considering that amino acids 68–132 are necessary but not sufficient for actin binding, an alternative possibility is that Yih1 dimerizes on actin, *i.e.* endogenous Yih1 stabilizes an interaction between the Yih1 fragment harboring part of the actin-binding site and the actin molecule(s). Finally, it is possible that an as yet unknown molecule facilitates the bridging of two Yih1 proteins, in a manner dependent on residues 68–171. Either way, these results raise the possibility that other factors may draw Yih1 into a complex with actin, in addition to the direct Yih1-actin interaction we uncovered previously (18).

A link between the cytoskeleton and translation in yeast has been suggested by the observations that a defect in the actin cytoskeleton affects protein synthesis and, conversely, that translation factors, *e.g.* eEF1, affect the integrity of the actin cytoskeleton (43–48). In addition, we have previously shown that a reduction in actin levels in a diploid strain in which one of the copies of the gene encoding actin was deleted (*ACT1*/*act1*) results in the inability of cells to activate Gcn2, and this was partially reverted by deleting *YIH1* (18). We have also shown that overexpression of GST-Yih1 exacerbated the Gcn^- phenotype of the *ACT1*/*act1* strain. Those findings indicated that Yih1 may provide a means for the cytoskeleton to spatially affect Gcn2 activation and thus protein synthesis (48). Our working model, derived from those studies and reinforced by the data shown here, is that free G-actin would bind to Yih1 allowing for Gcn2 activation. In specific locations in the cells, where actin is mainly polymerized, the resulting availability of free Yih1 would then sequester Gcn1 thus preventing Gcn2 activation. We have suggested previously that this is specifically relevant in the vicinity of the growing bud to ensure maximum protein synthesis. The increase in localized protein synthesis mediated by inhibition of Gcn2 may be required for the formation of the new cell.

Even though at least part, if not all, of the ancient domain in Yih1 was shown here to be required for actin binding, the UPF0029 motif alone was not sufficient for binding actin. We showed here that the UPF0029 domain contains several motifs of identical residues in all organisms, highlighting an extremely conserved function common to all living cells (25). However, no clues exist for the function of this domain, and there is no obvious phenotype imparted on cells by the lack of YigZ or Yih1 (18, 49), raising the possibility that its function is not required under laboratory conditions but is crucial under still unknown physiological conditions. Notably, our modeling provided evidence that the evolutionarily conserved motifs in Yih1 and YigZ are clustered on one side of the molecule (25), suggesting that the common feature of ancient domains is mediating interactions with a highly conserved cellular component (Fig. 10*A*, *right arrow*). We showed that these motifs harbor neighboring residues that are distinct for either the prokaryotic or the eukaryotic lineages, probably representing specificity determinants for their partners within these life domains. Given the involvement of Yih1 in modulating a ribosomal associated complex (Gcn1-Gcn2), it is possible that the UPF0029 domain binds to a ribosomal component.

Our model shown in Fig. 10, derived from this work, proposes that actin binding to Yih1 prevents Yih1 from efficiently disrupting Gcn1-Gcn2 interaction. The fact that Gcn1 is found in various complexes not containing Gcn2 suggests that Yih1 may interact with Gcn1 that is engaged in cellular processes other than Gcn2 regulation. Interestingly, cells harbor additional RWD domain proteins, such as Gir2/RWDDI in yeast/mammals, which was proposed to relay signals to or from Gcn1 (50–52). Thus it is tempting to speculate that Gcn1 and Yih1/IMPACT may play additional important roles in the cell apart from Gcn2 regulation.

Acknowledgments—We thank Kristina Blagoeva and Htin Aung for technical support; David Botstein, Thomas Dever, and Jan van't Riet for antibodies; and Martin Roffe and Michael Bolech for helpful comments on the manuscript.

REFERENCES

1. Dever, T. E. (2002) *Cell* **108,** 545–556
2. Hinnebusch, A. G. (2000) in *Translational Control of Gene Expression* (Sonenberg, N., Hershey, J. W., and Mathews, M. B., eds) pp. 185–243, Cold Spring Harbor Laboratory Press, Cold Spring Harbor, NY
3. Costa-Mattioli, M., Gobert, D., Harding, H., Herdy, B., Azzi, M., Bruno, M., Bidinosti, M., Ben Mamou, C., Marcinkiewicz, E., Yoshida, M., Imataka, H., Cuello, A. C., Seidah, N., Sossin, W., Lacaille, J. C., Ron, D., Nader, K., and Sonenberg, N. (2005) *Nature* **436,** 1166–1173
4. Fallarino, F., Grohmann, U., You, S., McGrath, B. C., Cavener, D. R., Vacca, C., Orabona, C., Bianchi, R., Belladonna, M. L., Volpi, C., Santamaria, P., Fioretti, M. C., and Puccetti, P. (2006) *J. Immunol.* **176,** 6752–6761
5. Hao, S., Sharp, J. W., Ross-Inta, C. M., McDaniel, B. J., Anthony, T. G., Wek, R. C., Cavener, D. R., McGrath, B. C., Rudell, J. B., Koehnle, T. J., and Gietzen, D. W. (2005) *Science* **307,** 1776–1778
6. Maurin, A. C., Jousse, C., Averous, J., Parry, L., Bruhat, A., Cherasse, Y., Zeng, H., Zhang, Y., Harding, H. P., Ron, D., and Fafournoux, P. (2005) *Cell Metab.* **1,** 273–277
7. Doerks, T., Copley, R. R., Schultz, J., Ponting, C. P., and Bork, P. (2002) *Genome Res.* **12,** 47–56
8. Sattlegger, E., and Hinnebusch, A. G. (2000) *EMBO J.* **19,** 6622–6633
9. Kubota, H., Sakaki, Y., and Ito, T. (2000) *J. Biol. Chem.* **275,** 20243–20246
10. Sattlegger, E., and Hinnebusch, A. G. (2005) *J. Biol. Chem.* **280,** 16514–16521
11. Marton, M. J., Crouch, D., and Hinnebusch, A. G. (1993) *Mol. Cell. Biol.* **13,** 3541–3556
12. Vazquez de Aldana, C. R., Marton, M. J., and Hinnebusch, A. G. (1995) *EMBO J.* **14,** 3184–3199
13. Marton, M. J., Vazquez de Aldana, C. R., Qiu, H., Chakraburtty, K., and Hinnebusch, A. G. (1997) *Mol. Cell. Biol.* **17,** 4474–4489
14. Nameki, N., Yoneyama, M., Koshiba, S., Tochio, N., Inoue, M., Seki, E., Matsuda, T., Tomo, Y., Harada, T., Saito, K., Kobayashi, N., Yabuki, T., Aoki, M., Nunokawa, E., Matsuda, N., Sakagami, N., Terada, T., Shirouzu, M., Yoshida, M., Hirota, H., Osanai, T., Tanaka, A., Arakawa, T., Carninci, P., Kawai, J., Hayashizaki, Y., Kinoshita, K., Güntert, P., Kigawa, T., and Yokoyama, S. (2004) *Protein Sci.* **13,** 2089–2100
15. Pereira, C. M., Sattlegger, E., Jiang, H. Y., Longo, B. M., Jaqueta, C. B.,

Hinnebusch, A. G., Wek, R. C., Mello, L. E., and Castilho, B. A. (2005) *J. Biol. Chem.* **280,** 28316–28323
16. Bittencourt, S., Pereira, C. M., Avedissian, M., Delamano, A., Mello, L. E., and Castilho, B. A. (2008) *J. Comp. Neurol.* **507,** 1811–1830
17. Hagiwara, Y., Hirai, M., Nishiyama, K., Kanazawa, I., Ueda, T., Sakaki, Y., and Ito, T. (1997) *Proc. Natl. Acad. Sci. U.S.A.* **94,** 9249–9254
18. Sattlegger, E., Swanson, M. J., Ashcraft, E. A., Jennings, J. L., Fekete, R. A., Link, A. J., and Hinnebusch, A. G. (2004) *J. Biol. Chem.* **279,** 29952–29962
19. Foiani, M., Cigan, A. M., Paddon, C. J., Harashima, S., and Hinnebusch, A. G. (1991) *Mol. Cell. Biol.* **11,** 3203–3216
20. Güldener, U., Heck, S., Fielder, T., Beinhauer, J., and Hegemann, J. H. (1996) *Nucleic Acids Res.* **24,** 2519–2524
21. Dever, T. E., Feng, L., Wek, R. C., Cigan, A. M., Donahue, T. F., and Hinnebusch, A. G. (1992) *Cell* **68,** 585–596
22. Mulholland, J., Preuss, D., Moon, A., Wong, A., Drubin, D., and Botstein, D. (1994) *J. Cell Biol.* **125,** 381–391
23. Sali, A., and Blundell, T. L. (1993) *J. Mol. Biol.* **234,** 779–815
24. Berman, H. M., Westbrook, J., Feng, Z., Gilliland, G., Bhat, T. N., Weissig, H., Shindyalov, I. N., and Bourne, P. E. (2000) *Nucleic Acids Res.* **28,** 235–242
25. Park, F., Gajiwala, K., Eroshkina, G., Furlong, E., He, D., Batiyenko, Y., Romero, R., Christopher, J., Badger, J., Hendle, J., Lin, J., Peat, T., and Buchanan, S. (2004) *Proteins* **55,** 775–777
26. Altschul, S. F., Gish, W., Miller, W., Myers, E. W., and Lipman, D. J. (1990) *J. Mol. Biol.* **215,** 403–410
27. Jones, D. T., Taylor, W. R., and Thornton, J. M. (1992) *Nature* **358,** 86–89
28. Thompson, J. D., Gibson, T. J., Plewniak, F., Jeanmougin, F., and Higgins, D. G. (1997) *Nucleic Acids Res.* **25,** 4876–4882
29. Bowie, J. U., Lüthy, R., and Eisenberg, D. (1991) *Science* **253,** 164–170
30. Laskowski, R. A., MacArthur, M. W., Moss, D. S., and Thornton, J. M. (1993) *J. Appl. Crystallogr.* **26,** 283–291
31. Emsley, P., and Cowtan, K. (2004) *Acta Crystallogr. D Biol. Crystallogr.* **60,** 2126–2132
32. Krissinel, E., and Henrick, K. (2004) *Acta Crystallogr. D Biol. Crystallogr.* **60,** 2256–2268
33. Holm, L., and Sander, C. (1994) *Proteins* **19,** 165–173
34. Murzin, A. G., Brenner, S. E., Hubbard, T., and Chothia, C. (1995) *J. Mol. Biol.* **247,** 536–540
35. Orengo, C. A., Michie, A. D., Jones, S., Jones, D. T., Swindells, M. B., and Thornton, J. M. (1997) *Structure* **5,** 1093–1108
36. Sonnhammer, E. L., Eddy, S. R., and Durbin, R. (1997) *Proteins* **28,** 405–420
37. Cutler, P. (1996) in *Protein Purification Protocols, Methods in Molecular Biology* (Doonan, S., ed) Vol. 59, pp. 255–268, Humana Press Inc., Totowa, NJ
38. Kubota, H., Ota, K., Sakaki, Y., and Ito, T. (2001) *J. Biol. Chem.* **276,** 17591–17596
39. Chen, Y. H., Yang, J. T., and Martinez, H. M. (1972) *Biochemistry* **11,** 4120–4131
40. Ghaemmaghami, S., Huh, W. K., Bower, K., Howson, R. W., Belle, A., Dephoure, N., O'Shea, E. K., and Weissman, J. S. (2003) *Nature* **425,** 737–741
41. Uetz, P., Giot, L., Cagney, G., Mansfield, T. A., Judson, R. S., Knight, J. R., Lockshon, D., Narayan, V., Srinivasan, M., Pochart, P., Qureshi-Emili, A., Li, Y., Godwin, B., Conover, D., Kalbfleisch, T., Vijayadamodar, G., Yang, M., Johnston, M., Fields, S., and Rothberg, J. M. (2000) *Nature* **403,** 623–627
42. Gavin, A. C., Bösche, M., Krause, R., Grandi, P., Marzioch, M., Bauer, A., Schultz, J., Rick, J. M., Michon, A. M., Cruciat, C. M., Remor, M., Höfert, C., Schelder, M., Brajenovic, M., Ruffner, H., Merino, A., Klein, K., Hudak, M., Dickson, D., Rudi, T., Gnau, V., Bauch, A., Bastuck, S., Huhse, B., Leutwein, C., Heurtier, M. A., Copley, R. R., Edelmann, A., Querfurth, E., Rybin, V., Drewes, G., Raida, M., Bouwmeester, T., Bork, P., Seraphin, B., Kuster, B., Neubauer, G., and Superti-Furga, G. (2002) *Nature* **415,** 141–147
43. Gross, S. R., and Kinzy, T. G. (2007) *Mol. Cell. Biol.* **27,** 1974–1989
44. Pittman, Y. R., Kandl, K., Lewis, M., Valente, L., and Kinzy, T. G. (2009) *J. Biol. Chem.* **284,** 4739–4747
45. Kandl, K. A., Munshi, R., Ortiz, P. A., Andersen, G. R., Kinzy, T. G., and Adams, A. E. (2002) *Mol. Genet. Genomics* **268,** 10–18
46. Munshi, R., Kandl, K. A., Carr-Schmid, A., Whitacre, J. L., Adams, A. E., and Kinzy, T. G. (2001) *Genetics* **157,** 1425–1436
47. Gross, S. R., and Kinzy, T. G. (2005) *Nat. Struct. Mol. Biol.* **12,** 772–778
48. Munn, A., and Sattlegger, E. (2009) *Aust. Biochemist* **40,** 9–13
49. Baba, T., Ara, T., Hasegawa, M., Takai, Y., Okumura, Y., Baba, M., Datsenko, K. A., Tomita, M., Wanner, B. L., and Mori, H. (2006) *Mol. Syst. Biol.* **2,** 2006.0008
50. Wout, P. K., Sattlegger, E., Sullivan, S. M., and Maddock, J. R. (2009) *Eukaryot. Cell* **8,** 1061–1071
51. Kang, N., Chen, D., Wang, L., Duan, L., Liu, S., Tang, L., Liu, Q., Cui, L., and He, W. (2008) *Cell. Mol. Immunol.* **5,** 333–339
52. Alves, V. S., and Castilho, B. A. (2005) *Biochem. Biophys. Res. Commun.* **332,** 450–455
53. DeLano, W. L. (2002) *The PyMOL Molecular Graphics System*, DeLano Scientific LLC, San Carlos, CA